

Condition assessment of reinforced concrete bridges using structural health monitoring techniques - A case study

E. Mehrani¹, A. Ayoub² and A. Ayoub^{3*}

¹*DCI Solutions Inc., Lutz, FL 33548, U.S.A.*

²*Dept. of Civil and Environmental Engineering, University of Houston, Houston, TX 77204, U.S.A.*

³*PBS&G, Tampa, FL 33607, U.S.A.*

(Received August 20, 2008, Accepted September 21, 2008)

Abstract. The paper presents a case study in which the structural condition assessment of the East Bay bridge in Gibsonton, Florida is evaluated with the help of remote health monitoring techniques. The bridge is a four-span, continuous, deck-type reinforced concrete structure supported on prestressed pile bents, and is instrumented with smart Fiber Optic Sensors. The sensors used for remote health monitoring are the newly emerged Fabry–Perot (FP), and are both surface-mounted and embedded in the deck. The sensing system can be accessed remotely through fast Digital Subscriber Lines (DSL), which permits the evaluation of the bridge behavior under live traffic loads. The bridge was open to traffic since March 2005, and the collected structural data have been continuously analyzed since. The data revealed an increase in strain readings, which suggests a progression in damage. Recent visual observations also indicated the presence of longitudinal cracks along the bridge length. After the formation of these cracks, the sensors readings were analyzed and used to extrapolate the values of the maximum stresses at the crack location. The data obtained were also compared to initial design values of the bridge under factored gravity and live loads. The study showed that the proposed structural health monitoring technique proved to provide an efficient mean for condition assessment of bridge structures providing it is implemented and analyzed with care.

Keywords: structural health monitoring; condition assessment; smart structures; fiber optic sensors; remote monitoring.

1. Introduction

Health monitoring of civil infrastructure systems has recently emerged as a powerful tool for condition assessment of structural performance. With the widespread use of modern telecommunication technologies, structures could now be monitored periodically from a central station located several miles away from the field. This remote capability allows immediate damage detection, so that necessary actions that ensure public safety are taken. Remote health monitoring can be performed using a variety of sensors and techniques. Strain gauges, accelerometers, LVDT, and inclinometers have all been used for this purpose. Fiber Optic Sensors have numerous advantages over conventional electrical resistance strain gauges and are therefore more suitable for strain monitoring, as discussed by Ansari (2005). The first known wireless accelerometer was developed by Straser and Kiremidjian (1998), and was known as the WiMMS system. Later, wireless communication techniques were expanded and used for different types

*Corresponding Author, E-mail: asayoub@uh.edu

of sensors, as discussed by Lynch and Loh (2005). In addition, miniature micro-electro-mechanical systems (MEMS) or smart dust sensors could be also used, as well as Piezoelectric sensors.

Many bridges worldwide have been instrumented with continuous monitoring systems. In the US, Idriss, *et al.* (1997), Catbas, *et al.* (1998), Aktan, *et al.* (2000), Hipley (2001), Sikorsky, *et al.* (2003), Wang (2004), Bastianini, *et al.* (2007), and Mehrani, *et al.* (2008) reported successful implementation of continuous monitoring of bridges. In addition, similar work was conducted in Canada by Mufti, *et al.* (1997), Choquet, *et al.* (1999), Cheung and Naumoski (2002), and Benmokrane, *et al.* (2006). Long term monitoring of bridges was also reported in China by Ou (2004) and Ko and Ni (2005); in Korea by Koh, *et al.* (2003) and Yun, *et al.* (2003); in Japan by Wu (2003) and Fujino and Abe (2004); and in Europe by Casciati (2003) and Brownjohn (2003).

The objective of this work is to present a case study, where the condition assessment of the reinforced concrete East Bay bridge in Hillsborough county, Florida is evaluated using remote health monitoring techniques with Fiber Optic sensors. The emphasis of the discussion is on the analysis of the collected data and their use in tracking crack initiation and propagation. The proposed health monitoring system is described in the next section.

2. Remote health monitoring system

The remote sensing system used in this study relies on Fabry-Perot Fiber Optic Sensors and consists of: 1) Fabry-Perot Sensors attached to critical locations of the structure, 2) Fiber Optic Cables to connect the FP sensors to their acquisition system, 3) Acquisition system securely housed on-site, and 4) DSL connection to remotely connect to the acquisition system.

3. Installation of health monitoring system on the East Bay Bridge

The original bridge was a concrete structure built in the early 1970s. The bridge was classified as functionally obsolete due to severe deck cracking, corrosion of the longitudinal bars, and its narrow width. The replacement bridge is a four-span 120' long and 55' wide structure and is shown in Fig. 1. The interior spans are 33' and the exterior spans are 27' long. The intermediate spans are continuous, and the middle span is fixed over the central bent. The superstructure is composed of 18" thick cast-in-



Fig. 1 Elevation view of the New East Bay Bridge

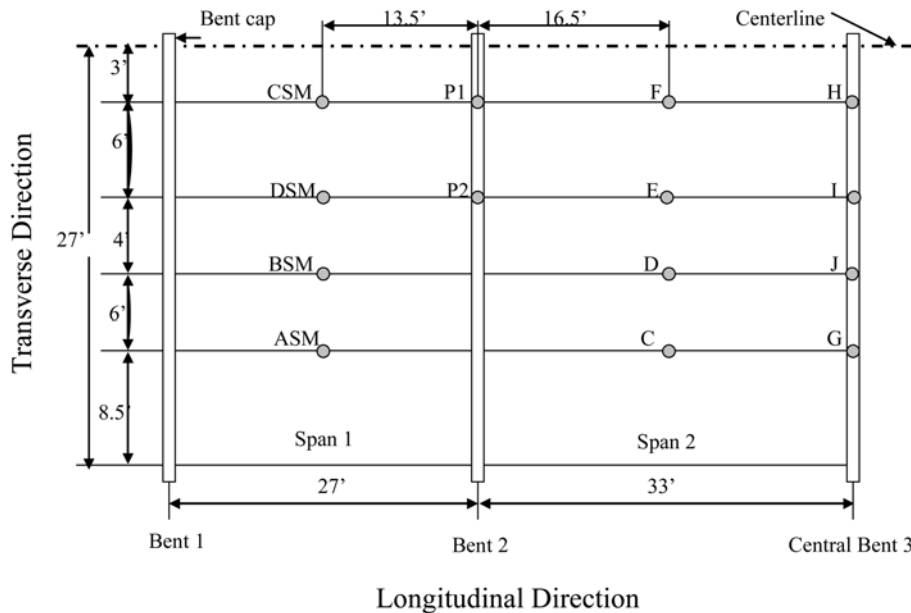


Fig. 2 Sensors location

Legend

1. Surface-mount sensors ASM, BSM, CSM, DSM: Bonded with epoxy to bottom deck
2. Surface-mount sensors P1 and P2: Bonded with epoxy to top deck
3. Embedded sensors C, D, E, F: Bonded to bottom reinforcing bars
4. Embedded sensors G, H, I, J: Bonded to top reinforcing bars

place reinforced concrete slab, while the substructure is composed of 24” square pre-stressed concrete piles. The top and bottom mats consisted of # 9 rebar (1.125” diameter) placed 6” on center. The clear space between the bars was 4.87”.

A total of sixteen Fabry-Perot strain sensors capable of measuring within a range of +/- 2000 $\mu\epsilon$ were installed on the bridge as part of the health monitoring system. Fig. 2 illustrates the position of the sensors along the bridge length. Three types of sensor are placed in four categories of installation. The three types of sensors are identified as 1) Surface mount, known as Fiso-B (blade), 2) Embedded sensors, and 3) Embedded temperature sensors. The location of these sensors along the deck thickness is identified in Fig. 3. Four embedded sensors were bonded to the bottom longitudinal reinforcing bars, and four blade sensors were surface-mounted to the concrete bottom deck surface. In addition, four embedded sensors were bonded to the top reinforcing bars over the bents, and two blade sensors were surface mounted to the concrete top deck surface. Two more sensors for temperature compensation were installed on the top and bottom bars respectively.

The sensors were carefully installed per the manufacturer’s recommendations, then wrapped in nitrite rubber. Fig. 4 shows a close view of the installation and wrapping process of sensors on reinforcing bars. The micro capillary section of sensors is glass and thus is very sensitive to scratch and impact. Also, optical fibers are very sensitive to bends, kinks, sharp curves and impact. To avoid damage to the system, the fiber optic cables were inserted into 1” diameter schedule-40 PVC pipes. The pipe conduits were guided through the crowded rebar mats to the edge of slab. The openings in the conduits were sealed with nitrate rubber sheet and caulking. The conduits were tightly secured to the rebars. Fig. 5

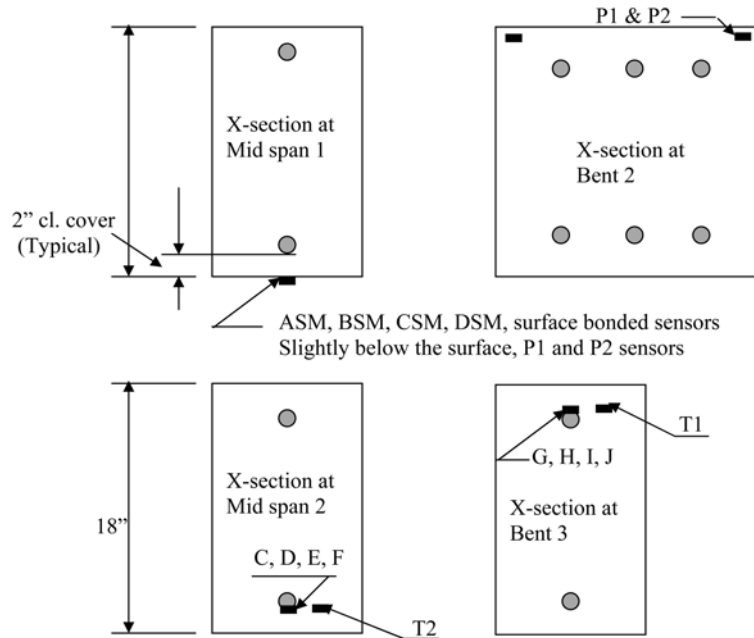


Fig. 3 Sensors location along thickness



Fig. 4 Installation of sensors on rebars

shows a plan view of the conduits within the rebar mats. The conduits containing the fiber optic cables were brought unto the forms of the slab. At this area, the fiber optic cables are most vulnerable to the construction activities such as worker's traffic and placing and removing the forms. A 2" diameter hole was drilled out to allow the conduit to exit the slab. Three small boxes (12"×12"×12") were fabricated to house the cables at the point of exit. The conduits were then guided to the smart box containing the acquisition system. The smart box was attached to the side of bridge and locked for security as shown in Fig. 6. The acquisition system weights only 10 lbs, and has dimensions of 17.7"×12.8"×5.2" and cost around \$14,000, which accounts for less than 1% of the overall cost of the bridge (\$1.5 millions). To access the acquisition system remotely, telephone and power lines that were buried 30" below the surface were brought to the bridge.



Fig. 5 PVC conduit protection



Fig. 6 Smart box on bridge side

The phone line serves to remotely access the smart box through fast DSL connections. The traffic data are currently being continuously collected and analyzed with the purpose of evaluating the bridge structural health. A more detailed description of the installation of the health monitoring system as well as the data collection and analysis is provided in Mehrani (2006).

4. Design of the East Bay Bridge

In order to conduct an accurate condition assessment of the bridge structural health, the collected data need to be compared to the corresponding values evaluated during the original design of the bridge. A brief description of the bridge design process is given in this section.

The Florida Department of Transportation standard specification for road and bridge construction and supplemental (2000) was used for the design of the bridge. The AASHTO LRFD method of design (2004) was used throughout. The design live load for LRFD method is HL-93 loading, which is the combination of a design truck or a design tandem with design uniform lane load. The Design truck load

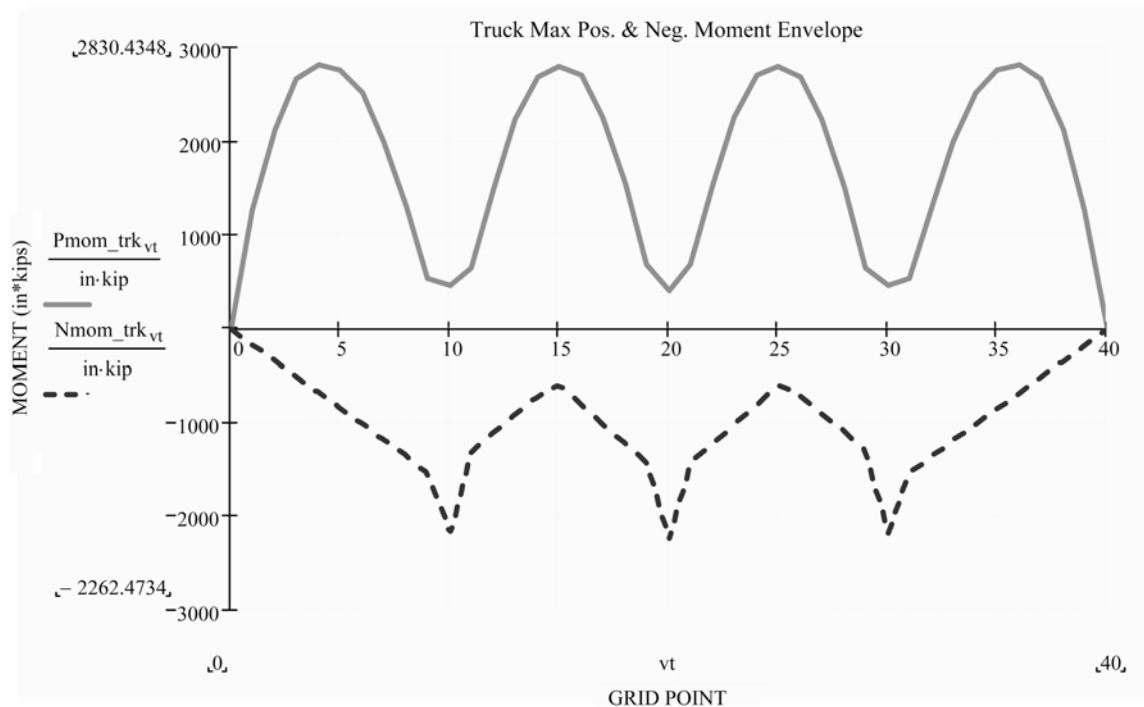


Fig. 7 Bending moments due to HS-20 truck loading

is HS20-44 truck, and the design tandem has each axle weighing 25 kips. The design truck load is increased by 1.33, which is the dynamic impact load allowance.

The Load Factor Design (LFD) method has been predominantly used in analysis of Bridge Load Rating. The LFD method was presented in the first edition, first printing, of AASHTO manual for maintenance inspection of bridges in July 1970. Since then, several editions have been printed, but there has not been any significant modification in the formulation and application.

The AASHTO manual for maintenance inspection of bridges requires highway bridges to be rated at two load levels, either by load factor or by working stress methods. At the first or upper level, rating is referred to as Operating Rating. The operating rating will result in the absolute maximum permissible load level to which the structure may be subjected to. At the second or lower level, rating is referred to as inventory rating. The inventory rating will result in a load level, which can safely utilize an existing structure of an indefinite period of time. To determine the Rating Factor, RF for the Operating Level, all six Florida legal trucks, SU2, SU3, SU4, C3, C4, C5, two design vehicles, HS20-44 and HL-93, and military loading must be investigated and the rating factor, RF for all nine cases must be evaluated.

The FDOT MathCAD-based live load generator (2005) was used to obtain all positive and negative moments for service live load. The dead load moment was obtained from beam analysis. The moment envelope for HS-20 truck is shown in Fig. 7. For design purpose, the notional design truck HL-93 is used. The corresponding service moments, cracked and uncracked section results are given below.

Table 2 Strains, ϵ , of uncracked section in micro-strain, $\mu\epsilon$

ϵ .	SU2	SU3	SU4	C3	C4	C5	HS20	HL-93
LL _{pos}	35.085	62.078	67.548	37.711	55.19	42.523	63.32	67.275
LL _{neg}	22.141	42.356	45.863	39.212	52.573	50.756	50.615	45.852
DL	36.51	36.51	36.51	36.51	36.51	36.51	36.51	36.51

5. Condition assessment of the East Bay Bridge

The East Bay bridge has been continuously monitored under the effect of traffic load since its opening in March 2005. Figs. (8a-b) show the strain values of sensor F as designated in Figs. 2 and 3 for two intervals during the first year of service, a reading recorded three months after initial operation and another one seven months later. The maximum value recorded for the first reading was $9.5 \mu\epsilon$ and

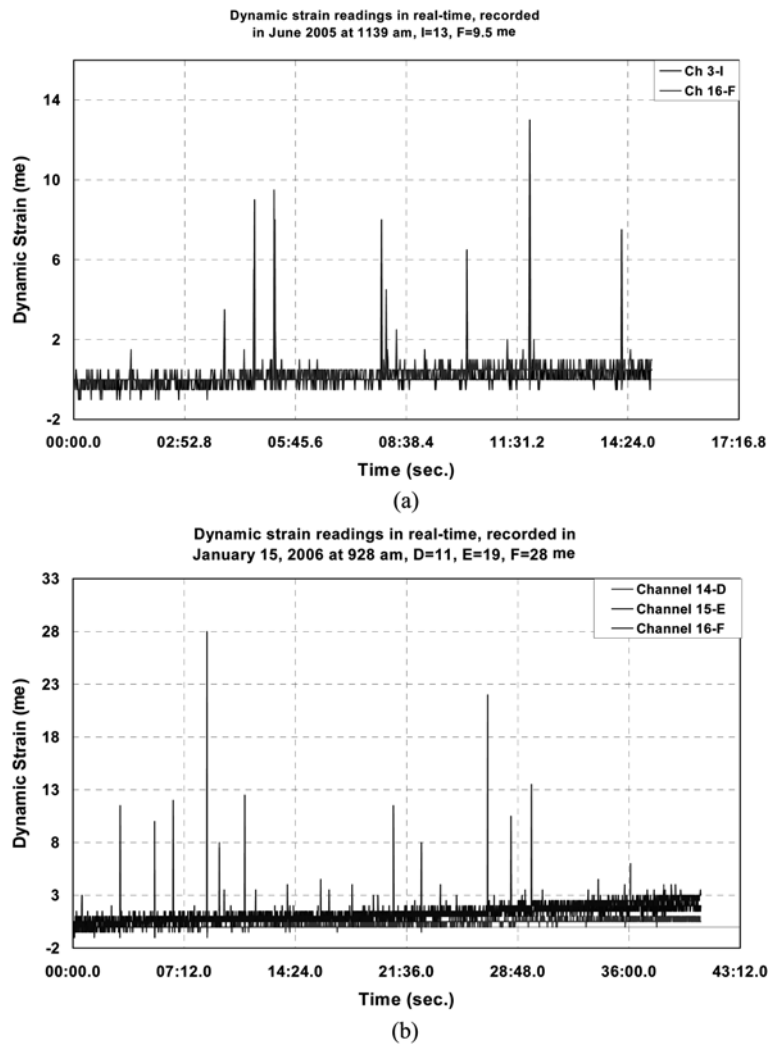


Fig. 8 (a) Dynamic strain 06/14/2005 ($\epsilon_{\max} = 9.5 \mu\epsilon$), (b) Dynamic strain 01/15/2006 ($\epsilon_{\max} = 28 \mu\epsilon$)



Fig. 9 1st crack on bottom of bridge deck

that of the second reading was $28 \mu\epsilon$. Progression in strain values were evident, although the recorded strain values as well as visual observations at that time indicated that there were no cracks present in the bridge deck underside.

By examining the maximum recorded strain data over the first 12-month period of operation, it was found that they agree well with the design values assuming uncracked conditions and reported in Table 2, rather than those of the cracked conditions shown in Table 1. Additional static and dynamic load tests, as well as finite element analysis of the bridge, were performed by Mehrani, *et al.* (2008) and resulted in the same conclusion. Such uncracked condition was not assumed in the original design of the bridge, which lead the authors to initially believe that current design guidelines are conservative.

However, recent visual observations revealed the presence of two discrete cracks on the bottom of the deck propagating along the length of the bridge as shown in Fig. 9. The transverse location of these cracks was approximately at 5ft and 11ft to the west of the centerline respectively. The longitudinal cracks are not believed to be due to splitting failure, since the detailing of the reinforcing bars within the concrete deck was carefully designed. The formation of the longitudinal cracks is more likely due to either restraining shrinkage effects which can result in curling of the deck, lack of concrete consolidation, or overstress in the transverse direction. The latter seems to be the most likely cause since the location of these two cracks is very close to that of the traveling wheel loads. In this case, the longitudinal cracks typically form at the bottom surface along the wheel path as the wheel loads move on the bridge deck in the longitudinal direction (Pedikaris, *et al.* 1993). A combination of overstress in the transverse direction and curling is also a possibility. In any case, these cracks pose concerns as they allow for the intrusion of water and chlorides that can potentially lead to corrosion of the reinforcement bars. A more detailed discussion on the different types of bridge deck cracks and their potential damage is given in NCHRP-380 (1996).

The maximum strain reading of sensor F recorded in August 2008 under the passage of heavy trucks, and after the observation of the longitudinal cracks, is shown in Fig. 10. The figure depicts a maximum value of strain of $42 \mu\epsilon$. Static loading of the bridge using SU-4 trucks was also performed in August 2008, and the recorded strain value of sensor F was equal to $45 \mu\epsilon$. While these values reveal a progression of damage, they do not suggest the presence of cracks, which contradicts the recent visual observations. However, to further understand this phenomena the following study is performed:

Consider a reinforced concrete member subjected to axial tension as shown in Fig. 11. In this case

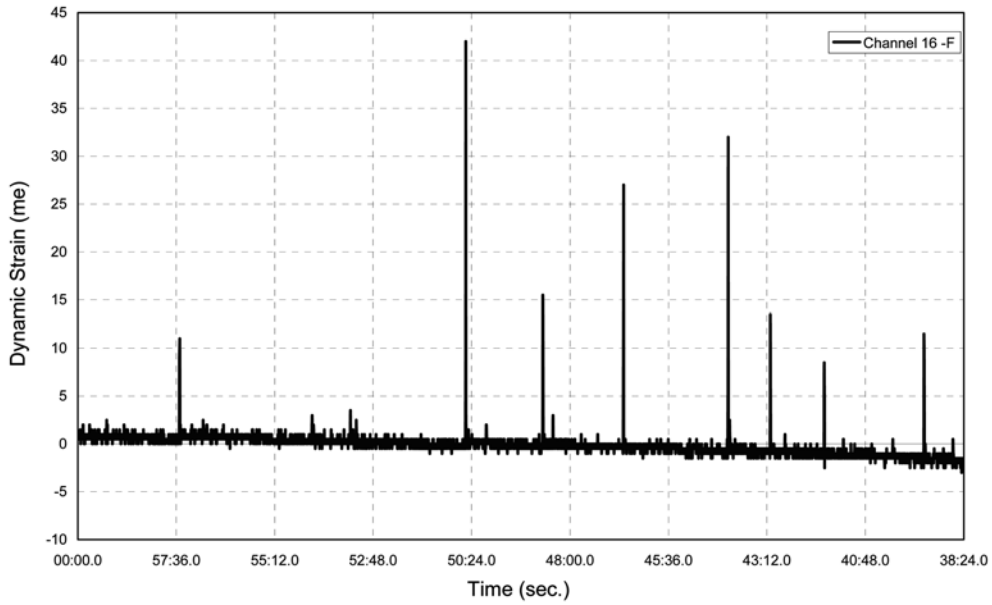


Fig. 10 Dynamic strain 08/14/2008 ($\epsilon_{\max} = 42 \mu\epsilon$)

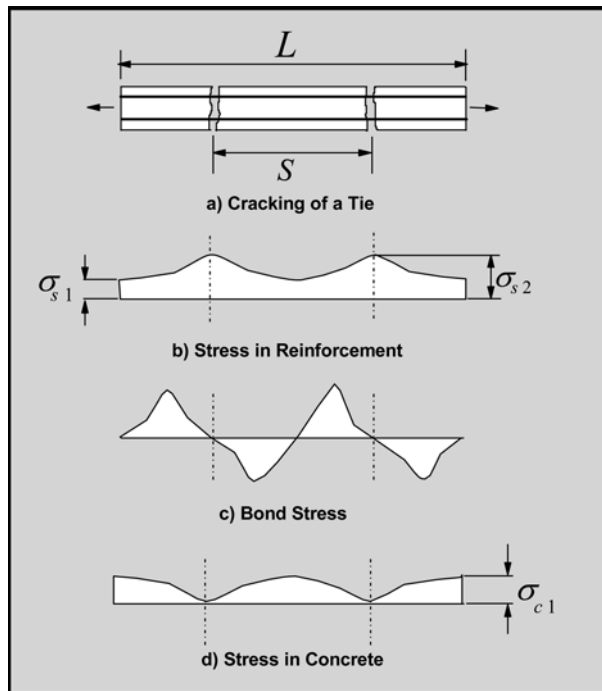


Fig. 11 Stresses at cracking

tensile stresses are transmitted across the crack through the bonded reinforcing steel. If the axial stress does not exceed the tensile strength of concrete, the member is ideally free of cracks. This state is referred to as state 1. The steel and concrete strains, ϵ_{s1} and ϵ_{c1} , respectively, are compatible along the

member. The average strain is:

$$\epsilon_{s1} = \epsilon_{c1} = \frac{N}{E_c(A_c + nA_s)} = \frac{N}{E_c A_1} \tag{1}$$

where N is the value of the axial force, A_c and A_s are the cross sectional areas of concrete and steel and $n = E_s/E_c$ with E_s and E_c being the moduli of elasticity of steel and concrete respectively. When the concrete stress exceeds the tensile strength, cracks appear. At a crack the stress is completely carried by the reinforcement and the concrete stress is zero. This condition will be referred to as state 2. The steel stress and strain are given by:

$$\sigma_{s2} = N/A_s \tag{2}$$

$$\epsilon_{s2} = N/E_s A_s \tag{3}$$

In the portion between two cracks, part of the tensile stress carried by the steel at the crack is transferred to the concrete through bond. The stress and strain are in an intermediate state between states 1 and 2, as depicted in Fig. 12. Midway between consecutive cracks, the section is in state 1 and the steel stress is less than σ_{s2} . At a crack the section is in state 2 with the steel stress at its maximum value σ_{s2} and with the concrete stress equal to zero. The difference in steel stress is transmitted to the concrete through bond, so that the member elongates less than the bare steel. Denoting the average or smeared strain of the cracked member in Fig. 11(a) as ϵ_m , then

$$\epsilon_m = \Delta L/L \tag{4}$$

where L is the original length of the member and ΔL is the member elongation.

Before cracking, compatibility of strains is maintained so that Eq. (1) holds ($\epsilon_m = \epsilon_{s1} = \epsilon_{c1}$). After cracking, the value of ϵ_m lies for a given stress level between the steel strain in the perfectly bonded case ϵ_{s1} and the steel strain at the crack ϵ_{s2} .

Denoting the reduction in steel strain due to the participation of concrete between cracks by $\Delta\epsilon$, then

$$\epsilon_m = \epsilon_{s2} - \Delta\epsilon \tag{5}$$

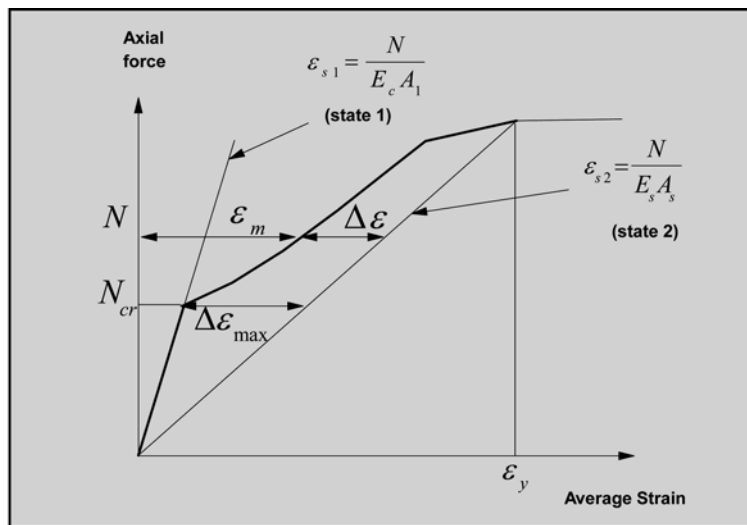


Fig. 12 Axial force vs. average strain for an axially loaded reinforced specimen

Based on experimental evidence, it is assumed that $\Delta\varepsilon$ varies inversely with the applied axial load N (CEB 1985):

$$\Delta\varepsilon = \Delta\varepsilon_{\max} \frac{N_{cr}}{N} \quad (6)$$

where N_{cr} is the cracking load and $\Delta\varepsilon_{\max}$ is the steel strain difference between states 1 and 2 at the first crack.

From the graph in Fig. 12:

$$\Delta\varepsilon_{\max} = (\varepsilon_{s2} - \varepsilon_{s1}) \frac{N_{cr}}{N} \quad (7)$$

Substitution of Eq. (6) in (7) gives the average strain value of the member:

$$\varepsilon_m = (1 - \zeta) \varepsilon_{s1} + \zeta \varepsilon_{s2} \quad (8)$$

where ζ is a dimensionless parameter that represents the amount of cracking and is given by:

$$\zeta = 1 - \left(\frac{N_{cr}}{N} \right)^2 \quad (9)$$

$\zeta = 0$ for an uncracked member. The difference between the solid line and the line representing the bare steel in Fig. 12 is referred to as tension stiffening. It represents the increase in stiffness due to the concrete contribution between cracks. Tension stiffening can be significant up to the yielding of the reinforcement, but drops considerably near the yield point. After yielding of the reinforcement at the most critical section, the member elongates without significant increase in load and the tension carried by the concrete becomes negligible.

The installed Fiber Optic sensors are either embedded and bonded to the rebars or surface-mounted to the concrete. The surface-mounted sensors would record the strain $\varepsilon_{c1} = \varepsilon_{s1}$ before cracking. After cracking, if the sensor is exactly located at the crack position, its reading will drop to zero. It is more likely, however, that the sensor exists between two cracks. In this case the reading of the sensor will drop, but to a non-zero value. Gradual decrease of the sensor readings indicate the formation of additional cracks until the deck becomes severely cracked. In this case, the readings will approach zero values. The role of the surface-mounted sensors therefore is to detect the formation of the initial cracks and to monitor the crack propagation with time. After the deck becomes severely cracked, these sensors won't be able to record service strain values.

The role of the embedded sensors on the other hand, is to monitor the service strain values in addition to recording the maximum steel stress values at cracked locations. Before cracking the sensors would record the strain $\varepsilon_{s1} = \varepsilon_{c1}$. When the strain ε_{c1} reaches the concrete cracking strains, this will indicate the formation of the first crack. The steel strain at the crack location will increase and reach the value of ε_{s2} , but the steel strain between cracks will be less than ε_{s2} . If the sensor is exactly located at the crack position, it will record the value of ε_{s2} . This is however unlikely to happen, and it is assumed that the sensor is recording an average value that equals ε_m as defined in Eq. (5). In order to extrapolate the value of the steel strain at the crack location, Eq. (8) is used to estimate the value of the axial force N resisted by the reinforced concrete section, which is again used with the help of Eq. (3) to evaluate the steel strain at the crack location ε_{s2} . A further increase in the value of either ε_m or ε_{s2} under the same loading conditions indicate the formation of additional cracks or a decrease in the value of the crack spacing S identified in Fig. 11.

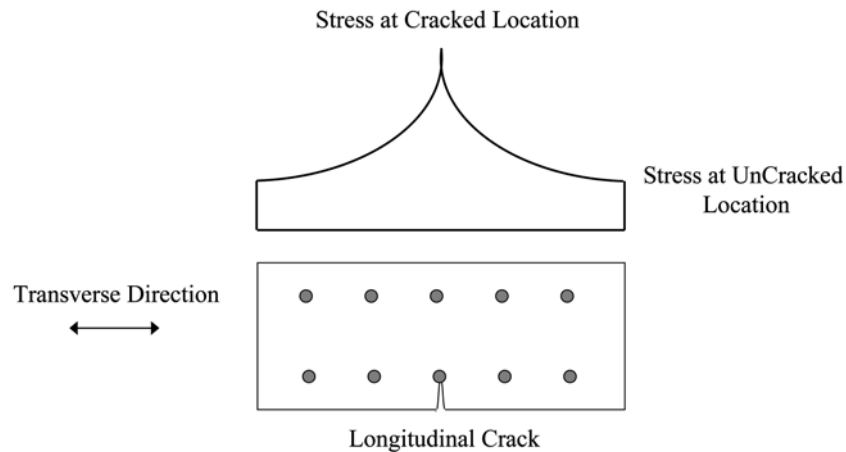


Fig. 13 Stress distribution of cracked section

The previous equations are typically used to extrapolate the maximum steel strain at the cracked location after initial cracking of the section. For the case of the East Bay bridge, due to the presence of the longitudinal cracks that were probably formed because of high flexural stresses in the transverse direction, the stress distribution at a section in the longitudinal direction is expected to be as shown in Fig. 13. In this case, the stresses in the bars at the crack location are maximum, while those in the bars away from the crack are minimum. The equations derived earlier could still be used to evaluate the average section strain. Since the load that caused the longitudinal crack to form is unknown, it is assumed that it is the one that corresponds to the last recorded strain value before cracking ($28 \mu\epsilon$). From Eq. (1), $N_{cr} = 82.08$ kips. Assuming the maximum recorded strain to be the averaged smeared strain $\epsilon_m = 45 \mu\epsilon$, Eq. (8) can be used to solve for the only unknown N , which can substituted in Eqs. (1), (3) and (9) to evaluate ϵ_{s1} , ϵ_{s2} and ζ . The solution resulted in the following values: $\epsilon_{s1} = 31 \mu\epsilon$, $\epsilon_{s2} = 118 \mu\epsilon$, and $\zeta = 0.165$. These values suggest that even though the maximum recorded strain was $45 \mu\epsilon$, the expected maximum strain at the crack location is actually $118 \mu\epsilon$, which exceeds the cracking strain of concrete. This observation suggests that the assumption of cracked conditions used in the initial design matches well with the current condition of the bridge. The strain value at the crack location matches better with the design strains evaluated in Table 1 assuming cracked conditions, than with those evaluated assuming uncracked conditions.

The preceding discussion confirms that the continuous monitoring with Fiber Optic Sensors can provide a good mean for condition assessment of bridges providing its results are analyzed with care. Periodic visual inspection is still necessary in order to capture the different types of damage that could not be directly interpreted from the sensors readings. The sensors data however could be extrapolated and used to track crack initiation and propagation, and more importantly to monitor the steel stress increase following crack initiation.

6. Conclusions

The paper presents a case study for the application of continuous monitoring with Fiber Optic Sensors for condition assessment of reinforced concrete bridge structures. A total of sixteen Fabry-

Perot Fiber Optic sensors were installed on the East Bay bridge, in Hillsborough County, Florida. The sensors were both bonded to the longitudinal reinforcing bars and surface-mounted to the concrete deck. The sensors data were transmitted to the bridge maintenance office through DSL lines. The bridge was continuously monitored since its opening in March 2005. The data obtained were compared to initial design values of the bridge under factored gravity and live loads. The collected data over this period revealed a progression of damage due to the increase in strain readings. Recent visual observations however indicated the presence of two longitudinal cracks along the bridge length. While the sensors could not directly predict the formation of these discrete cracks, simple analysis could be used to extrapolate the stresses at the crack location from the sensors readings. The study showed that the continuous monitoring with Fiber Optic Sensors proved to provide an efficient mean for condition assessment of bridge structures providing its results are analyzed with care. The sensors data can in general be used to track crack propagation, and to monitor the steel stress increase following crack initiation.

Acknowledgements

The authors would like to acknowledge the support of Hillsborough County staff members, formers and present, Mr. Bernardo Garcia, Mr. Robert Gordon, Mr. Larry Watts, and Mr. Wayne Miller.

References

- AASHTO (1970), *Manual for maintenance inspection of bridges*, American Association of State Highway and Transportation Officials, Washington, D.C.
- AASHTO (1978), *Manual for maintenance inspection of bridges*, American Association of State Highway and Transportation Officials, Washington, D.C.
- AASHTO (2004), *LRFD bridge design specifications*, third edition, American Association of State Highway and Transportation Officials, Washington, D.C.
- Aktan, A.E., Grimmelsman, K.A., Barrish, R.A., Catbas, F.N. and Tsikos, C.J. (2000), *Structural identification of a long span truss bridge*, TRR No. 1696, National Academy Press, Washington D.C., 210-218.
- Ansari, F. (2005), "Sensing issues in civil structural health monitoring", *Proc. of NSF Workshop in Civil Structural Health Monitoring*, Springer publishing, 527.
- Bastianini, F., Matta, F., Rizzo, A., Galati, N. and Nanni, A. (2007), "Overview of recent bridge monitoring applications using distributed brillouin fiber optic sensors", *Nondestruct. Test.*, **12**(9), 269-276.
- Benmokrane, B., El-Salakawy, E.F., ElRagaby, A., Lackey, T. and Desgagné, G. (2006), "Design and testing of concrete bridges reinforced with glass FRP bars", *J. Bridge Eng. ASCE*, **11**(2), 217-229.
- Brownjohn, J.M.W. (2003), "Lessons from monitoring the performance of highway bridges", *Proc. of the Int. Workshop on Advanced Sensors, Structural Health Monitoring and Smart Structures*.
- Casciati, F. (2003), "An overview of structural health monitoring expertise within the European Union", *Structural Health Monitoring and Intelligent Infrastructure*, Lisse, Balkema, 31-37.
- Catbas, F.N., Lenett, M., Aktan, A.E., Brown, D.L., Helmicki, A.J. and Hunt, V. (1998), "Damage detection and condition assessment of seymour bridge", *Proc. of the 16th Int. Modal Analysis Conf.*, Santa Barbara, California.
- CEB (1985), "Cracking and deformations", Bulletin D'information No. 158, Comite Euro-International du Beton, Paris, France.
- Cheung, M.S. and Naumoski, N. (2002), "The first smart long-span bridge in Canada - health monitoring of the confederation bridge", *Proc. of the 1st Int. Workshop on Structural Health Monitoring of Innovative Civil Engineering Structures*, Winnipeg, Canada, 31-44.
- Choquet, P., Juneau, F. and Dadoun, F. (1999), "New generation of Fiber-Optic sensors for dam monitoring",

- Presented at the '99 Int. Conf. on Dam Safety and Monitoring, Three Gorge Project Site, Yichang, Hubei, China.
- Florida Department of Transportation (2000), *Standard specification for road and bridge construction and supplemental*.
- Fujino, Y. and Abe, M. (2004), "Structural health monitoring—current status and future", *Proc. of the 2nd European workshop on structural health monitoring*, Lancaster, 3-10.
- Hipley, P. (2001), "Caltrans' current state-of-practice", *Proc. of Instrumental Systems for Diagnostics of Seismic Response of Bridges and Dams*, Richmond, CA, 3-7.
- Idriss, R.L., Kersey, A.D. and Davis, M. (1997), "Highway bridge monitoring using optical fiber sensors", *Geotechnical News*, **15**(1), 43-45.
- Ko, J.M. and Ni, Y.Q. (2005), "Technology developments in structural health monitoring of large-scale bridges", *Eng. Struct.*, **27**, 1715-1725.
- Koh, H.M., Choo, J.F., Kim, S.K. and Kim, C.Y. (2003), "Recent application and development of structural health monitoring systems and intelligent structures in Korea", *Structural Health Monitoring and Intelligent Infrastructure*, Lisse, Balkema, 99-111.
- Krauss, P.D. and Rogalla, E.A. (1996), "Transverse cracking in newly constructed bridge decks", NCHRP Report No. 380, Transportation Research Board, National Report Council, Washington D. C., 126.
- LRFD Live Load Generator Version 2.41 (2005), Florida Department of Transportation.
- Lynch, J.P. and Loh, K. (2005), "A summary review of wireless sensors and sensor networks for structural health monitoring", *Shock Vib.*, **38**(2), 91-128.
- MathCAD 11 (2002), Mathsoft Engineering & Education, Inc.
- Mehrani, E. (2006), "Evaluation of AASHTO design specifications for cast-in-place continuous bridge decks using remote sensing techniques", Ph.D. Dissertation, University of South Florida.
- Mehrani, E., Ayoub, A.S. and Ayoub, A. (2008), "Evaluation of fiber optic sensors for remote health monitoring of bridge structures", *J. Mater. Struct.*, in press and available online.
- Mufti, A.A., Tadros, G. and Jones, P.R. (1997), "Field assessment of fiber-optic bragg grating strain sensors in the confederation bridge", *Can. J. Civil Eng.*, **24**, 963-966.
- Ou, J. (2004), "The state-of-the-art and application of intelligent health monitoring systems for civil infrastructures in mainland of China", *Progress in Structural Engineering, Mechanics and Computation*, London, 599-608.
- Perdikaris, P.C., Petrou, M.F. and Wang, A. (1993), "Fatigue strength and stiffness of reinforced concrete bridge decks", Final Report to ODOT, FHWA/OH-93/016, Dept. of Civil Eng., Case Western Reserve, Cleveland Ohio.
- Sikorsky, C., Stubbs, N. and Karbhari, V. (2003), "Automation of damage index method to evaluate structural safety", *Proc. of the Thirteenth Int. Offshore and Polar Engineering Conf.*, Honolulu, Hawaii.
- Straser, E.K. and Kiremidjian, A.S. (1998), "A Modular, wireless damage monitoring system for structures", Report No. 128, The John A. Blume Earthquake Engineering Center, Stanford University.
- Wang, M.L. (2004), "State-of-the-art applications in health monitoring", *Workshop on Basics of Structural Health Monitoring and Optical Sensing Technologies in Civil Engineering*, Taiwan, National Central University, 113-142.
- Wu, Z.S. (2003), "Structural health monitoring and intelligent infrastructures in Japan", *Proc. of the 1st Int. Conf. Structural Health Monitoring and Intelligent Infrastructure*, Tokyo, Japan, **1**, 153-167.
- Yun, C.B., Lee, J.J., Kim, S.K. and Kim, J.W. (2003), "Recent R & D activities on structural health monitoring for civil infra-structures in Korea", *KSCE J. Civil Eng.*, **7**(6), 637-651.